Biomedical Signal Processing and Control 18 (2015) 56–60

Contents lists available at ScienceDirect

Biomedical Signal Processing and Control

journal homepage: www.elsevier.com/locate/bspc

Characterizing gait asymmetry via frequency sub-band components of the ground reaction force

B.L. Su [a], R. Song [b], L.Y. Guo [c], C.W. Yen [a,d,*]

[a] Department of Mechanical and Electro-mechanical Engineering, National Sun Yat-Sen University, Kaohsiung, Taiwan
[b] School of Engineering, Sun Yat-Sen University, Guangzhou, China
[c] Department of Sports Medicine, Kaohsiung Medical University, Kaohsiung, Taiwan
[d] Department of Physical Therapy, Kaohsiung Medical University, Kaohsiung, Taiwan

ARTICLE INFO

Article history:
Received 9 February 2014
Received in revised form
25 September 2014
Accepted 10 November 2014
Available online 29 December 2014

Keywords:
Gait analysis
Gait asymmetry
Wavelet transform
Ground reaction force

ABSTRACT

This study introduces gait asymmetry measures by comparing the ground reaction force (GRF) features of the left and right limbs. The proposed features were obtained by decomposing the GRF into components of different frequency sub-bands via the wavelet transform. The correlation coefficients between the right and left limb GRF components of the same frequency sub-band were used to characterize the degree of bilateral symmetry. The asymmetry measures were then obtained by subtracting these coefficients from one. To demonstrate the effectiveness of these asymmetry measures, the proposed measures were applied to differentiate the walking patterns of Parkinson's patients and healthy subjects. The results of the statistical analyses found that the patient group has a higher degree of gait asymmetry. By comparing these results with those obtained by conventional asymmetry measures, it was found that the proposed approach can more effectively distinguish the differences between the tested Parkinson's disease patients and the healthy control subjects.

1. Introduction

As an indispensable element of daily activity, gait is a complex motor skill governed by several inter-linked pathways. A possible approach that can help us understand the mechanism behind limb coordination in generating the gait motion is to study gait asymmetry (GA). Despite the fact that the symmetry of normal walking remains a controversial issue [1,2], many studies have demonstrated that marked GA appears in many pathological conditions. For example, studies have found that limb length discrepancy [3], stroke [4], cerebral palsy [5] and Parkinson's disease (PD) [6] may result in a significantly asymmetrical gait because bilateral differences in the support time, stride length, ground reaction force (GRF), muscle moments or joint motion have been detected for these patients.

The asymmetrical gait features that have been studied can be divided into two categories: (1) discrete parameters, such as swing time [7] and stride length [8], and (2) continuous signals, such as joint displacement [9], GRF [10] and electromyography [11] signals. Compared with the discrete parameters, a distinct advantage of the continuous signals is that they can be analyzed by both time and frequency domain methods. As a result, one can often extract more information from these gait signals to study GA.

In comparison with other continuous gait signals, a distinct property of the GRF is that the acceleration of the center of mass (COM) of the body is directly proportional to GRF. As a result, many features can be extracted from GRF to differentiate healthy and abnormal gait patterns. For example, the diagnostic potentials of GRF for pathological gaits have been demonstrated for ankle arthrodesis [12], hip arthroplasty [13], patellofemoral pain syndrome [14], multiple sclerosis [15] and peripheral arterial disease [16], etc. However, little attention has been given to the development of GRF-based asymmetry measures to detect gait abnormalities.

Parkinson's disease (PD) is one of the most common age-related neurodegenerative disorders and is expected to impose an increasing burden as society ages [17,18]. Initializing early therapy by early diagnosis is considered to be very important for the management of PD [19]. It is also believed that early diagnosis of PD can pave the way for major advances in disease-modifying therapies [20]. Unfortunately, the diagnosis of PD still remains mainly clinical and is very difficult in the early stages of the disease [21]. Hence, many

* Corresponding author at: Department of Mechanical and Electro-mechanical Engineering, National Sun Yat-Sen University, Kaohsiung, Taiwan.
Tel.: +886 73482965; fax: +886 75254299.
E-mail address: cmurobot@gmail.com (C.W. Yen).

http://dx.doi.org/10.1016/j.bspc.2014.11.008
1746-8094/

physiological signal based computer-aided-diagnosis (CAD) methods have been proposed to help physicians to make better diagnostic decisions. Since most important symptoms of PD include muscle rigidity, tremors and changes in speech and gait, these CAD methods often extract features from muscle activity [22–24], acoustic signal [25–27] or gait motion [28–30] to discriminate patients with PD. Among these CAD methods, gait based techniques are uniquely challenging and valuable for several reasons. First, early gait dysfunction can be subtle and non-specific and is often erroneously ascribed to old age or medical conditions such as osteoarthritis. This is very likely the reason why PD patients presenting with gait disturbance experienced the longest diagnostic delay [31]. Second, gait difficulty has been shown to be a predictor of decreased survival in PD [32]. Therefore, by characterizing the severity of gait dysfunction with quantified measures, these CAD methods have the potential to improve the treatment of PD by monitoring the progression of gait disorder.

Quantitative gait differences between normal subjects and PD patients have been discussed since 1980s [33,34]. In 1990s, several studies have investigated the stride length and stride time differences between PD and normal subjects [35–39]. Due to the disruption of neuromuscular control of gait, PD is characterized by asymmetric motor deficits in both the upper and lower extremities [40]. Consequently, later studies have tried to compare the degree of GA between PD patients and healthy subjects. For example, it has been shown that PD patients have larger asymmetry in swing time [6,7] and arm swing magnitude [41] than healthy individuals. Since gait analysis can produce a large number of features to characterize abnormal gait patterns, recent studies have tried to develop PD diagnostic methods by combining multiple number of gait features such as walking speed, peak flexion of the knee joint and ankle displacement [42–45]. However, most of these approaches focus on the kinematic parameters of the gait. Relatively few studies have tried to use the kinetic features such as GRF to diagnose PD patients [46,47].

The aim of this work is to introduce GA measures by performing time-frequency spectral analysis on the GRF signals via the wavelet transform. It is hypothesized that the degree of asymmetry of the wavelet-decomposed GRF signal components of the pathological gaits is larger than that of the normal gaits. The validity of this hypothesis will be tested by comparing the proposed GA measures between the PD patients and the healthy control subjects.

The gait dataset studied in this work is obtained from Physionet [48]. The vertical component of the GRF (VGRF) was measured as the test subjects walked at their usual, self-selected pace for approximately 2 min. The sampling rate was chosen as 100 Hz. The original form of the data included eight VGRF components measured by eight sensors located at different spots under the foot. The VGRF was obtained by totaling the outputs of these eight sensors and then dividing by the weight of the tested subject. The original dataset consists of 93 PD patients (58 males and 35 females) and 73 healthy subjects (40 males and 33 females). However, two male and two female PD patients and one healthy male subject were not included in this study because of the lack of weight data.

2. Methods

2.1. Measurements

This study focuses on VGRF which is the force component with the largest magnitude that the ground impacts on the body. Fig. 1 shows a typical M-shape VGRF profile of a normal walking gait [49]. Three characteristic points can be identified from such a VGRF profile. As shown in Fig. 1, this standard walking VGRF profile exhibits two peaks. The first peak (F_1) corresponds to the period right after

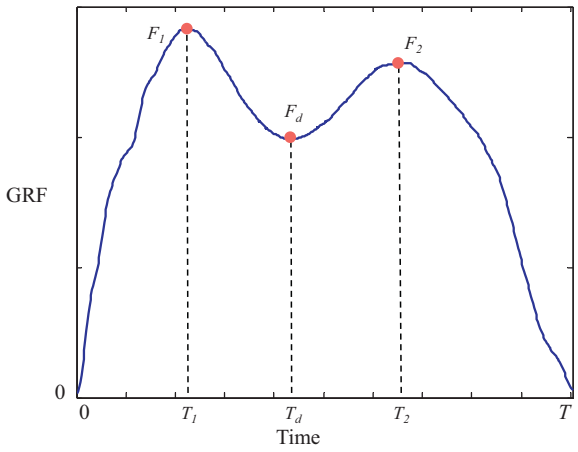

Fig. 1. A typical walking GRF profile.

the heel strike when the center of gravity is moving downward, resulting in an increased VGRF. The second peak (F_2) occurs when the person applies a force to the ground which is then matched by an increase in the VGRF. The dip (F_d) that comes between these two peaks occurs when the COM is rising up, thus decreasing the force of the body on the ground and resulting in the reduction of the VGRF. As shown in Fig. 1, the times of occurrence of F_1, F_2 and F_d are denoted as T_1, T_2 and T_d, respectively, and T is the time length of the step. In addition, every VGRF signal used in this study was normalized by dividing the outputs of the GRF sensors with the weight of the tested subject.

Because the swing and stance phases of a gait cycle can be detected by inspecting the magnitude of the GRF signal, one can easily determine step time, stance time, swing time and double stance time from the measurements of the GRF. The capability of deriving these important temporal gait features is also an advantage of GRF measurements.

Typically, gait asymmetry measures are developed by comparing the gait features of the left and right limbs. For the discrete parameter features, one of the most commonly employed GA measures is

$$GA = \frac{|X_L - X_R|}{2|X_L + X_R|}$$

where X_R and X_L are the values of the discrete parameter feature measured from the right and left limbs, respectively. The discrete parameter features studied in this work include the temporal features stance time, swing time, double stance time and the dynamic features $F_1, F_2, F_d, F_1/T_1$ (loading rate) and $F_3/(T - T_2)$ (push-off rate). Note that all these features can be derived from the GRF.

In addition to the discrete parameters, this study also performs a bilateral comparison for the VGRF signals. To achieve this goal, a VGRF signal was decomposed into a number of sub-band components via the wavelet transform. Compared with the traditional Fourier-based methods, which directly decomposes a signal into an infinite number of sinusoidal components of different frequencies, the wavelet transform has the following distinct advantages. First, wavelet methods can systematically decompose a complicated signal into a finite number of frequency sub-band components, which can be independently studied. Second, by using basis functions localized in time and frequency, the wavelet transform provides a systematic framework for analyzing the non-stationary signals. Third, the wavelet transform uses a window with a variable time size to process the signal. As a result, a good frequency resolution at low frequencies and a good time resolution at high frequencies can be simultaneously achieved. In contrast, the traditional Fourier

Table 1
Summary of asymmetry measures of the tested discrete parameters.

Features	Patients	Controls	p-Values	AUC
Step time	0.012 ± 0.004	0.010 ± 0.003	1.47E−04	0.67
Stance time	0.031 ± 0.010	0.028 ± 0.008	3.25E−02	0.60
Double stance time	0.012 ± 0.004	0.010 ± 0.003	1.92E−04	0.66
F_1	0.034 ± 0.019	0.024 ± 0.011	2.63E−04	0.66
F_d	0.046 ± 0.030	0.037 ± 0.018	2.23E−02	0.57
F_2	0.046 ± 0.031	0.040 ± 0.028	2.10E−01	0.56
F_1/T_1	0.093 ± 0.056	0.083 ± 0.041	2.07E−01	0.55
$F_2/(T-T_3)$	0.092 ± 0.039	0.090 ± 0.037	6.60E−01	0.52

method employs a fixed window size and thus has fixed time and frequency resolutions.

By using the wavelet transform, this work progressively decomposed the GRF signal into components of different frequency bands by using complementary low-pass and high-pass filters. Initially, the decomposed low and high frequency signal components were denoted as A_1 and D_1, respectively. The A_1 component was further decomposed into low (A_2) and high (D_2). In this recursive manner, this work decomposed the GRF signals into four levels of details D_1–D_4 and to one final approximation A_4. The actual frequency range of these low and high frequency components depends on the choice of the wavelet function. Since finding the most appropriate wavelet function for a given signal processing problem remains a research challenge, this work tested a number of wavelet functions. These wavelet functions include Biorthogonal 4.4 (bior4.4), Symlets 4, 9 (sym4, sym9), Coiflets 1 (coif 1), Coiflets 4 (coif 4), and Daubechies 11, 12, 13, 14, 15 and 16(db11,. . ., db16). For a more complete illustration of this signal decomposition process, readers are referred to two excellent tutorial papers on wavelet transform [50,51].

To evaluate the effectiveness of the tested wavelet functions in generating features for comparative GA studies, each of the tested wavelet functions was used to decompose the VGRF signals. The degree of symmetry was quantified by the Pearson product-moment correlation coefficient between the bilateral signal components of the same frequency sub-band. The corresponding asymmetry measure α was defined as $1-C$ with C denoting the correlation coefficient. Since the value of a Pearson correlation coefficient ranges from −1 to 1, the value of the proposed asymmetry measure α varies from 0 to 2 with a 0 representing a perfect symmetry, a 1 indicating no linear relation and a 2 signifying a perfect negative correlation between the bilateral signal components.

This study uses C_i to represent the correlation coefficient between the D_i components of the right and left legs, the corresponding asymmetry measure was denoted as α_i. Similarly, the asymmetry measure between the A_4 components of both sides was denoted as α_0. Finally, to demonstrate the differences made by the wavelet transform, the results obtained by the asymmetry measure (denoted as α^*) of the original VGRF profiles were also computed.

2.2. Statistical and classification methods

For the statistical analyses performed in this work, all hypotheses were non-directional and the critical significance level was 0.05. A two-sample t-test was used to detect statistically significant differences between the asymmetry measures of the patient and control groups.

To further compare the efficacy of the GA measures, each of these GA measures was used to independently classify the PD patient and healthy control groups. In particular, we formulated a binary classification problem for each of the tested GA measures by assigning PD patients as the positive class and the healthy subjects as the negative class. In solving such a binary classification problem, if the value of the tested GA measure of a subject is larger than a specified threshold, then the classifier considered the result to be positive and the subject was classified as a patient. Otherwise, the classification rule considered the result to be negative and the subject was classified as healthy.

If a PD patient is classified as positive, it was counted as a true positive. Otherwise, this PD patient was counted as false negative. Similarly, if a healthy subject is classified as negative, it was counted as a true negative. Otherwise, this healthy individual was counted as false positive. Apparently, the true and false positive rates of the classification results vary with the value of the threshold. By sweeping the threshold from the most positive to the most negative value, one can generate a receiver operating characteristic (ROC) curve by plotting the true positive rate as a function of the false positive rate. Because the area under the curve (AUC) of the ROC represents an estimate of the probability that the classifier ranks a randomly chosen positive example higher than a negative example, it has been considered to be a good performance index for classification methods [52].

The final part of our experimental study tried to use different combinations of features to differentiate PD patients. To achieve this goal, this study used the conventional back-propagation method to train multilayer perceptron (MLP) neural network models to learn to classify the PD patients and the healthy control subjects. In conducting the training process, 80%, 10% and 10% of the dataset was randomly divided into training, validation and test subsets, respectively. The training subset was used to generate optimal connection weights for the neural network models. The error of the validation subset was monitored by the early stop method to prevent overfitting. The test subset was used to evaluate the generalization performances of the MLP. This process was repeated 100 times and the average results of the test subset are reported.

2.3. Results

Table 1 summarizes the means and standard deviations of the GA measures for the tested discrete parameter features. In addition, Table 1 also provides the p-value and AUCs for these features. Note that an AUC of one represents a perfect classification, whereas a 0.5 is equivalent to random guessing. The differences between the proposed GA measures of the patient and control groups were also compared using t-tests, and the resulting p-values are summarized in Table 2 for every level of GRF components of all tested wavelet functions. The decomposition level was selected as four since further decomposition could not produce smaller p-value and failed to improve the classification accuracy. As demonstrated by Table 2, the resulting p-values are all smaller than 0.05 which clearly indicate that the differences of these GA measures between patient and control groups are statistically significant.

Table 3 summarizes the AUCs of three proposed GA measures with the smallest p-values among all results of Table 2. These three GA measures are the α_4 of Symlets 9, α_4 of Daubechies 14 and α_4 of Coiflets 1. Note that the results associated with α^*, which is the GA measure between the undecomposed bilateral VGRF profiles,

Table 2
Summary of the *p*-values of the *t*-test which is used to assess the differences of the proposed asymmetry measures between the patient and control groups.

Wavelet function	GRF components of different frequency sub-bands				
	A_4	D_4	D_3	D_2	D_1
bior4.4	2.83E−04	1.53E−06	1.30E−04	1.08E−03	1.68E−03
sym4	1.28E−04	3.86E−06	8.16E−05	4.33E−04	1.58E−03
sym9	5.14E−04	4.06E−10	2.72E−03	9.44E−04	3.13E−03
coif1	1.93E−04	1.67E−09	4.37E−07	1.48E−07	2.12E−06
coif4	1.44E−03	4.18E−04	2.35E−08	3.41E−03	2.08E−03
db4	3.45E−04	7.71E−04	4.82E−06	2.50E−04	2.79E−02
db11	3.07E−03	1.59E−07	1.51E−05	1.82E−03	1.23E−02
db12	3.75E−03	6.49E−08	2.28E−05	6.40E−04	4.57E−03
db13	4.74E−03	1.97E−09	1.56E−06	3.83E−03	2.19E−03
db14	6.46E−03	1.63E−09	1.15E−05	1.67E−03	2.15E−03
db15	6.15E−03	3.26E−06	1.6E−06	2.78E−04	3.06E−03
db16	6.36E−03	4.15E−06	1.98E−05	2.20E−03	4.72E−03

are also given in Table 3. Among these four features, the best accuracy was obtained by α_4 of Coiflets 1 which yielded an accuracy level of 0.720, a sensitivity score of 0.854 and a positive predictive value (PPV) of 0.704. Considering the possibility that the diagnostic efficacy can be further improved by combining multiple features to perform classification, we have tried to use every possible combinations of the features of Table 3 to solve the same classification problem. With an accuracy level of 0.862, a sensitivity score of 0.801 and a PPV of 0.931, the highest accuracy was obtained by the combination of α_4 of Symlets 9 and α_4 of Daubechies 14. These results compare favorably with two recent results of [46] (accuracy 0.733, sensitivity 0.811, PPV 0.881) and [47] (accuracy 0.711, sensitivity 0.702, PPV 0.711).

3. Discussion

The goal of this work is to develop a GRF-based GA measures to distinguish healthy and abnormal gaits. In contrast with many previous studies which only compared the GA for discrete parameter features, such as stance time, that only assess the temporal properties of the gait, this study focuses on the GA of the GRF-based features. As a consequence, the proposed method can assess the temporal as well as the dynamic properties of human gait.

To simultaneously analyze the GRF signal in time and frequency domains, this study employed the wavelet transform to decompose the GRF signal into components of different frequency sub-bands. These signal components were then used as gait features whose GA measures can be obtained by subtracting one from the correlation coefficients between the bilateral GRF signal components of the same frequency sub-band.

To demonstrate the potential of these wavelet-based GRF features, the asymmetry measures of the proposed features and some of the popular conventional gait features were used to assess the GA differences between the PD patient and healthy control groups. As demonstrated by the results of Table 1, at a significant level of 0.05, five of the eight tested discrete parameter features can effectively discriminate the GA differences between the PD patient and healthy control groups. Furthermore, as shown by the means of these measures, the patient group has a higher level of GA. This is in agreement with the results of previous studies which indicate that pathological conditions can deteriorate the symmetry of the walking motion.

The discrete parameter features tested in this work consist of two categories. The first three rows of Table 1 are temporal features which include step, stance and double stance times. The remaining discrete parameter features listed in Table 1 are dynamic features because they can be directly acquired from the GRF profile. As shown by the results of Table 1, asymmetry measures of the tested temporal features have smaller *p*-values and larger AUCs than those of the tested dynamic features.

In general, the low and high frequency signal components correspond, respectively, to the global shape and detailed variation of the signal. In this work, A_4 is the lowest frequency component whereas D_1 and D_2 are the two highest frequency components of the GRF signal. As shown by Table 2, the most effective GA measures are all associated with the D_3 or D_4 components. Such results can be explained by examining the means of the tested GA measures. For example, for the db14 wavelet function, the GA measure values for the A_4, D_4, D_3, D_2 and D_1 components of the healthy subjects are 0.011, 0.288, 0.561, 0.798 and 0.792, respectively. In comparison, the GA measure values for the A_4, D_4, D_3, D_2 and D_1 components of the PD patients are 0.015, 0.486, 0.723, 0.868 and 0.869, respectively. In addition to showing that the degree of GA increases with the frequency, these results also show that D_1 and D_2 components of the healthy subjects are already highly asymmetrical. As a consequence, there is relatively little room left for the PD to worsen the degree of symmetry. For the A_4 component, the GA measure of the healthy subjects and PD patients are 0.011 and 0.015, respectively. This indicates that the global shape of the GRF signal is highly symmetrical and relatively insensitive to PD. In contrast, relatively large symmetry declines occur at D_3 and D_4 components for the PD patients.

By comparing the *p*-values and AUCs of Tables 1 and 3, it is evident that the proposed wavelet generated GRF features clearly outperform the tested discrete parameter features in differentiating the GA between the patient and control groups. The results of Table 3 also demonstrate the impacts made by the wavelet transform. Specifically, the wavelet-decomposed components yielded smaller *p*-values and higher AUCs than the original VGRF signal in distinguishing the GA differences between PD and control groups.

Table 3
The asymmetry measures of the GRF profile and asymmetry measures from three GRF components that have the three smallest *p*-values among the results of Table 2.

Asymmetry measures	Patients	Controls	*p*-Values	AUC
α_4 of sym9	0.737 ± 0.364	0.426 ± 0.208	4.06E−10	0.75
α_4 of db14	0.486 ± 0.254	0.288 ± 0.124	1.63E−09	0.76
α_4 of coif1	0.357 ± 0.196	0.194 ± 0.094	1.67E−09	0.78
α^* of the VGRF profile	0.025 ± 0.012	0.016 ± 0.008	1.20E−06	0.74

One of the limitations of this work is that it only investigates the GRF in the vertical direction. While such a simplification can reduce the cost and complexity of instrumentation devices, it may be worthwhile to extend the GRF asymmetry study to the anterior-posterior and right-left directions. Another possibility is to use the proposed GA measures to monitor the effects of rehabilitation. The potential utilities of the proposed GA measures for early and differential diagnoses and for tracking the progression of diseases that may deteriorate the walking ability are also possible future research topics.

In summary, by using the wavelet transform to decompose the VGRF signals, this work introduced and tested a number of gait features to assess the GA differences between normal and pathological gaits. The experimental results demonstrate the effectiveness of the proposed approach by showing that the degree of asymmetry of the wavelet-decomposed gait GRF signal components of the PD patients is larger than that of the healthy persons. It is believed that the potential of the proposed GA measures can be explored in many clinical applications.

References

[1] H. Sadeghi, P. Allard, F. Prince, H. Labelle, Symmetry and limb dominance in able-bodied gait: a review, Gait Posture 12 (2000) 34–45.
[2] F.P. Carpes, C.B. Mota, I.E. Faria, On the bilateral asymmetry during running and cycling – a review considering leg preference, Phys. Ther. Sport 11 (2010) 136–142.
[3] J.R. Perttunen, E. Anttila, J. Södergård, J. Merikanto, P.V. Komi, Gait asymmetry in patients with limb length discrepancy, Scand. J. Med. Sci. Sports 14 (2004) 49–56.
[4] P.Y. Lin, Y.R. Yang, S.J. Cheng, R.Y. Wang, The relation between ankle impairments and gait velocity and symmetry in people with stroke, Arch. Phys. Med. Rehabil. 87 (2006) 562–568.
[5] R. White, I. Agouris, E. Fletcher, Harmonic analysis of force platform data in normal and cerebral palsy gait, Clin. Biomech. 20 (2005) 508–516.
[6] G. Yogev, M. Plotnik, C. Peretz, C.N. Giladi, J.M. Hausdorff, Gait asymmetry in patients with Parkinson's disease and elderly fallers: when does the bilateral coordination of gait require attention? Exp. Brain Res. 177 (2007) 336–346.
[7] R. Baltadjieva, N. Giladi, L. Gruendlinger, C. Peretz, J.M. Hausdorff, Marked alterations in the gait timing and rhythmicity of patients with de novo Parkinson's disease, Eur. J. Neurosci. 24 (2006) 1815–1820.
[8] D.S. Reisman, H. McLean, J. Keller, K.A. Danks, A.J. Bastian, Repeated split-belt treadmill training improves post stroke step length asymmetry, Neurorehabil. Neural Repair 27 (2013) 460–468.
[9] R.T. Roemmich, A.M. Field, J.M. Elrod, E.L. Stegemöller, M.S. Okun, C.J. Hass, Interlimb coordination is impaired during walking in persons with Parkinson's disease, Clin. Biomech. 28 (2013) 93–97.
[10] J.L. Riskowski, T.J. Hagedorn, A.B. Dufour, M.T. Hannan, Functional foot symmetry and its relation to lower extremity physical performance in older adults: the Framingham Foot Study, J. Biomech. 45 (2012) 1796–1802.
[11] R.A. Miller, M.H. Thaut, G.C. McIntosh, R.R. Rice, Components of EMG symmetry and variability in parkinsonian and healthy elderly gait, Electroencephalogr. Clin. Neurophysiol. 101 (1996) 1–7.
[12] W.L. Wu, F.C. Su, Y.M. Cheng, Y.L. Chou, Potential of the genetic algorithm neural network in the assessment of gait patterns in ankle arthrodesis, Ann. Biomed. Eng. 29 (2001) 83–91.
[13] J.L. McCrory, S.C. White, R.M. Lifeso, Vertical ground reaction forces: objective measures of gait following hip arthroplasty, Gait Posture 14 (2001) 104–109.
[14] D.T. Lai, P. Levinger, R.L. Begg, W.L. Gilleard, M. Palaniswami, Automatic recognition of gait patterns exhibiting patellofemoral pain syndrome using a support vector machine approach, IEEE Trans. Inf. Technol. Biomed. 13 (2009) 810–817.
[15] S.R. Wurdeman, J.M. Huisinga, M. Filipi, N. Stergiou, Multiple sclerosis affects the frequency content in the vertical ground reaction forces during walking, Clin. Biomech. 26 (2001) 207–212.
[16] D. McGrath, T.N. Judkins, I.I. Pipinos, J.M. Johanning, S.A. Myers, Peripheral arterial disease affects the frequency response of ground reaction forces during walking, Clin. Biomech. 27 (2012) 1058–1063.
[17] D. Twelves, K.S. Perkins, C. Counsell, Systematic review of incidence studies of Parkinson's disease, Mov. Disord. 18 (2003) 19–31.
[18] L.M. de Lau, M.M. Breteler, Epidemiology of Parkinson's disease, Lancet Neurol. 5 (2006) 525–535.
[19] C. Gallagher, E.B. Montgomery Jr., Early detection of Parkinson's disease, Handb. Clin. Neurol. 83 (2007) 457–477.
[20] S. Sharma, C.S. Moon, A. Khogali, A. Haidous, A. Chabenne, C. Ojo, M. Jelebinkov, Y. Kurdi, M. Ebadi, Biomarkers in Parkinson's disease (recent update), Neurochem. Int. 63 (2013) 201–229.
[21] E. Saracchi, S. Fermi, L. Brighina, Emerging candidate biomarkers for Parkinson's disease: a review, Aging Dis. 5 (2013) 27–34.
[22] E. Bakstein, J. Burgess, K. Warwick, V. Ruiz, T. Aziz, J. Stein, Parkinsonian tremor identification with multiple local field potential feature classification, J. Neurosci. Methods 209 (2012) 320–330.
[23] G. Rigas, A.T. Tzallas, M.G. Tsipouras, P. Bougia, E.E. Tripoliti, D. Baga, D.I. Fotiadis, S.G. Tsouli, S. Konitsiotis, Assessment of tremor activity in the Parkinson's disease using a set of wearable sensors, IEEE Trans. Inf. Technol. Biomed. 16 (2012) 478–487.
[24] B.K. Scanlon, B.E. Levin, D.A. Nation, H.L. Katzen, A. Guevara-Salcedo, C. Singer, S. Papapetropoulos, An accelerometry-based study of lower and upper limb tremor in Parkinson's disease, J. Clin. Neurosci. 20 (2013) 827–830.
[25] B. Walsh, A. Smith, Basic parameters of articulatory movements and acoustics in individuals with Parkinson's disease, Mov Disord. 27 (2012) 843–850.
[26] C.E. Stepp, Relative fundamental frequency during vocal onset and offset in older speakers with and without Parkinson's disease, J. Acoust. Soc. Am. 133 (2013) 1637–1643.
[27] W.L. Zuoa, Z.Y. Wanga, T. Liua, H.L. Chen, Effective detection of Parkinson's disease using an adaptive fuzzy k-nearest neighbor approach, Biomed. Signal Process. Control 4 (2013) 364–373.
[28] S.L. Chien, S.Z. Lin, C.C. Liang, Y.S. Soong, S.H. Lin, Y.L. Hsin, C.W. Lee, S.Y. Chen, The efficacy of quantitative gait analysis by the GAITRite system in evaluation of parkinsonian bradykinesia, Parkinsonism Relat. Disord. 12 (2006) 438–442.
[29] M.R. Daliri, Chi-square distance kernel of the gaits for the diagnosis of Parkinson's disease, Biomed. Signal Process. Control 8 (2013) 66–70.
[30] J. Klucken, J. Barth, P. Kugler, J. Schlachetzki, T. Henze, F. Marxreiter, Z. Kohl, R. Steidl, J. Hornegger, B. Eskofier, J. Winkler, Unbiased and mobile gait analysis detects motor impairment in Parkinson's disease, PLOS ONE 8 (2013) e56956.
[31] D.P. Breen, J.R. Evans, K. Farrell, C. Brayne, R.A. Barker, Determinants of delayed diagnosis in Parkinson's disease, J. Neurol. 260 (2013) 1978–1981.
[32] R.Y. Lo, C.M. Tanner, K.B. Albers, A.D. Leimpeter, R.D. Fross, A.L. Bernstein, V. McGuire, C.P. Quesenberry, L.M. Nelson, S.K. Van Den Eeden, Clinical features in early Parkinson disease and survival, Arch. Neurol. 66 (2009) 1353–1358.
[33] M.P. Murray, Studies of normal and abnormal locomotion, Int. J. Rehabil. Res. 2 (1979) 510–511.
[34] F. Handford, Parkinsonian gait, Physiotherapy 72 (1986) 341–342.
[35] O. Blin, A.M. Ferrandez, G. Serratrice, Quantitative analysis of gait in Parkinson patients: increased variability of stride length, J. Neurol. Sci. 98 (1990) 91–97.
[36] M.E. Morris, R. Iansek, T.A. Matyas, J.J. Summers, The pathogenesis of gait hypokinesia in Parkinson's disease, Brain 117 (1994) 1169–1181.
[37] J.C.M. Zijlmans, P.J.E. Poels, J. Duysens, J. Straaten, T. Thien, M.A. Van't Hof, H.O. Thijssen, M.W. Horstink, Quantitative gait analysis in patients with vascular Parkinsonism, Mov. Disord. 11 (1996) 501–508.
[38] J.M. Hausdorff, M.E. Cudkowicz, R. Firtion, J.Y. Wei, A.L. Goldberger, Gait variability and basal ganglia disorders: stride-to-stride variations of gait cycle timing in Parkinson's disease and Huntington's disease, Mov. Disord. 13 (1998) 428–437.
[39] M. Morris, R. Iansek, T. Matyas, J. Summers, Abnormalities in the stride length-cadence relation in parkinsonian gait, Mov. Disord. 13 (1998) 61–69.
[40] R. Djaldetti, I. Ziv, E. Melamed, The mystery of motor asymmetry in Parkinson's disease, Lancet Neurol. 5 (2006) 796–802.
[41] M.D. Lewek, R. Poole, J. Johnson, O. Halawa, X. Huang, Arm swing magnitude and asymmetry during gait in the early stages of Parkinson's disease, Gait Posture 31 (2010) 256–260.
[42] M.R. Daliri, Automatic diagnosis of neuro-degenerative diseases using gait dynamics, Measurement 45 (2012) 1729–1734.
[43] M. Galli, V. Cimolin, M.F. De Pandis, M.H. Schwartz, G. Albertini, Use of the gait deviation index for the evaluation of patients with Parkinson's disease, J. Mot. Behav. 44 (2012) 161–167.
[44] Y. Sarbaz, M. Banaie, M. Pooyan, S. Gharibzadeh, F. Towhidkhah, A. Jafari, Modeling the gait of normal and Parkinsonian persons for improving the diagnosis, Neurosci. Lett. 16 (2012) 72–75.
[45] U. Dillmann, C. Holzhoffer, Y. Johann, S. Bechtel, S. Gräber, C. Massing, J. Spiegel, S. Behnke, J. Bürmann, A.K. Louis, Principal component analysis of gait in Parkinson's disease: relevance of gait velocity, Gait Posture 39 (2014) 882–887.
[46] S.H. Lee, J.S. Lim, Parkinson's disease classification using gait characteristics and wavelet-based feature extraction, Expert Syst. Appl. 15 (2012) 7338–7344.
[47] S.E. Rodrigo, C.N. Lescano, R.H. Rodrigo, Application of Kohonen maps to kinetic analysis of human gait, Rev. Bras. Eng. Biom. 28 (2012) 217–226.
[48] A.L. Goldberger, L.A.N. Amaral, L. Glass, J.M. Hausdorff, P.C. Ivanov, R.G. Mark, J.E. Mietus, G.B. Moody, C.K. Peng, H.E. Stanley, PhysioBank, PhysioToolkit, and PhysioNet: components of a new research resource for complex physiologic signals, Circulation 101 (2000) e215–e220.
[49] V. Racic, A. Pavic, J.M.W. Brownjohn, Experimental identification and analytical modelling of human walking forces: literature review, J. Sound Vib. 326 (2009) 1–49.
[50] M. Unser, A. Aldroubi, A review of wavelets in biomedical applications, Proc. IEEE 84 (1996) 626–638.
[51] A.N. Akansua, W.A. Serdijnc, I.W. Selesnickb, Emerging applications of wavelets: a review, Phys. Commun. 3 (2010) 1–18.
[52] T. Fawcett, An introduction to ROC analysis, Pattern Recognit. Lett. 27 (2006) 861–874.